Morphological and Functional Diversity of the Mandible in Suckermouth Armored Catfishes (Siluriformes: Loricariidae)

Nathan K. Lujan* and Jonathan W. Armbruster

Department of Biological Sciences, Auburn University, Auburn, Alabama 36849

ABSTRACT We examined the mandibles of 377 individuals representing 25 species, 12 genera, 5 tribes, and 2 subfamilies of the Loricariidae, a species-rich radiation of detritivorous–herbivorous neotropical freshwater fishes distinguished by having a ventral oral disk and jaws specialized for surface attachment and benthic feeding. Loricariid mandibles are transversely oriented and bilaterally independent, each rotating predominantly around its long axis, although rotational axes likely vary with mandibular geometry. On each mandible, we measured three traditional and three novel morphological parameters chosen primarily for their functional relevance. Five parameters were linear distances and three of these were analogous to traditional teleost in- and out-levers for mandibular adduction. The sixth parameter was insertion area of the combined adductor mandibulae muscle (AM_{area}), which correlated with adductor mandibulae volume across a subset of taxa and is interpreted as being proportional to maximum force deliverable to the mandible. Multivariate analysis revealed distributions of phylogenetically diagnosed taxonomic groupings in mandibular morphospace that are consistent with an evolutionary pattern of basal niche conservatism giving rise to multiple adaptive radiations within nested clades. Correspondence between mandibular geometry and function was explored using a 3D model of spatial relationships among measured parameters, potential forces, and axes of rotation. By combining the model with known loricariid jaw kinematics, we developed explicit hypotheses for how individual parameters might relate to each other during kinesis. We hypothesize that the ratio [AM_{area}/tooth row length^2] predicts interspecific variation in the magnitude of force entering the mandible per unit of substrate contacted during feeding. Other newly proposed metrics are hypothesized to predict variation in aspects of mandibular mechanical advantage that may be specific to Loricariidae and perhaps shared with other herbivorous and detritivorous fishes. J. Morphol. 273:24–39, 2012.

KEY WORDS: evolutionary novelty; functional morphology; jaw diversity; jaw mechanics; durophagy; model

INTRODUCTION

The Loricariidae (Siluriformes: Loricarioidei) is a species-rich radiation of benthic herbivores and detritivores that are broadly distributed across the tropical freshwaters of South America and southern Central America. The over 800 known species in Loricariidae (Reis et al., 2003) are readily distinguished from other fishes by having bodies armored with ossified dermal plates and by having a specialized, ventrally positioned oral disk (Fig. 1). The loricariid oral disk encloses a highly mobile, tooth-bearing upper jaw comprising medially fused premaxillae and a lower jaw comprising independent, medially separated mandibles (Figs. 2 and 3). Each mandibular ramus is constructed of a medial, tooth-bearing dento-mentomeckelium (dentary) fused to a lateral anguloarticular. The anguloarticular receives most of the adductor mandibulae muscle and has a prominent lateral condyle, allowing the mandible to rotate around its long axis within a shallow socket at the anteroventral corner of the quadrate (Geerinckx et al., 2007a). Loricariid upper and lower jaw elements are adpressed to substrates via attachment of the oral disk and can be abducted at least 180° and then adducted rostrocaudally toward each other to scrape, gouge, pry, or winnow benthic food items that include flocculant detritus, algae, wood, and invertebrates.

Loricariidae is the most derived family in the neotropical-endemic superfamily Loricarioidei, within which an evolutionary series of biomechanical jaw decouplings has been described (Schaefer and Lauder, 1986). Trichomycteridae, the most basal loricarioid family, appear to represent a plesiomorphic condition in which mandibles are medially linked and premaxillae are either fused to the mesethmoid or have some mobility but no muscle insertion. Callichthyidae and Astroblepidae, which are lineages between Trichomycteridae and Loricariidae, have highly mobile premaxillae lacking

Additional Supporting Information may be found in the online version of this article.

*Correspondence to: Nathan K. Lujan, Department of Wildlife and Fisheries, Texas A&M University, MS 2258, College Station, TX 77840-2258. E-mail: nklujan@gmail.com

Received 13 December 2010; Revised 31 May 2011;
Accepted 15 June 2011

Published online 30 September 2011 in
Wiley Online Library (wileyonlineliberay.com)
DOI: 10.1002/jmor.11003

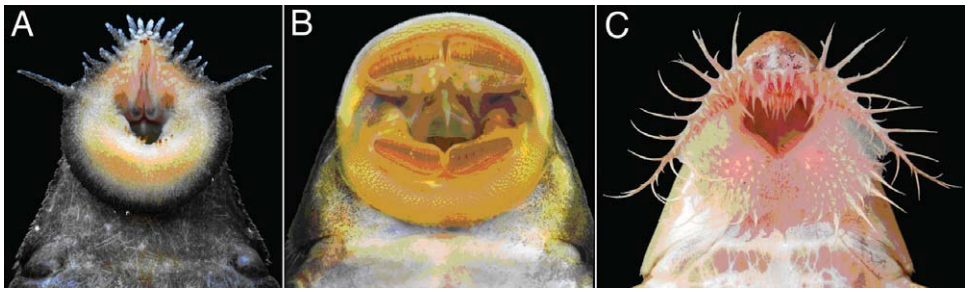

Fig. 1. Examples of loricariid oral disks: **A**: *Leporacanthicus* cf. *galaxias*, **B**: *Pseudancistrus sidereus*, and **C**: *Loricaria birindellii*. Photos by M. Sabaj Pérez.

direct muscle insertion, but only the latter more-derived family has bilaterally independent mandibles. Loricariidae, which is sister to Astroblepidae, is the only loricarioid lineage with a novel division of the adductor mandibulae inserting directly on the premaxilla. In addition to increasing upper and lower jaw kinesis, biomechanical decouplings in Loricarioidei may have permitted increased rates of morphological diversification via the removal of constraints on evolutionary freedom (Lauder, 1982; Schaefer and Lauder, 1986). A study quantifying morphological diversity across small subsamples of the four loricarioid families above found support for this hypothesis by correlating increased cranial morphological diversity with extent of jaw decoupling (Schaefer and Lauder, 1996); however, the small taxonomic range of this study (eight species per family) likely underrepresented total diversity across each of the sampled clades.

Knowledge of jaw morphological variation across the Loricariidae comes mostly from character descriptions in taxonomic and phylogenetic studies; fine-scale patterns of jaw morphological and correlated ecological diversity remain largely undescribed. Gross external features of loricariid trophic morphology, such as tooth row angle, tooth length, number, size, and cusp shape, have been described and associated with dietary specializations, but only among species-poor paraphyletic assemblages and only in a qualitative or nonstandardized manner (Delariva and Agostinho, 2001; Fugi et al., 2001; Mérona et al., 2008). Recent studies of loricariid ontogenetic series have provided detailed descriptions of jaw osteology and myology, but only qualitatively and for few taxa (Geerinckx, 2006; Geerinckx et al., 2007a). Unfortunately, quantitative description of jaw osteological diversity across a broader range of Loricariidae is complicated by the small size, complex three-dimensional shape, and morphological diversity of these elements (Fig. 4).

In this study, we focus on putatively functionally relevant morphometrics (e.g., lever arms and muscle insertion area) as an alternative to anatomical landmarks known or hypothesized to be developmentally homologous across all taxa. Our hypotheses of functional relevance are based primarily on qualitative aquarium observations and on the only study quantifying gross aspects of a single loricariid species' jaw motion (Adriaens et al., 2009). Adriaens et al. showed that rotation of the loricar-

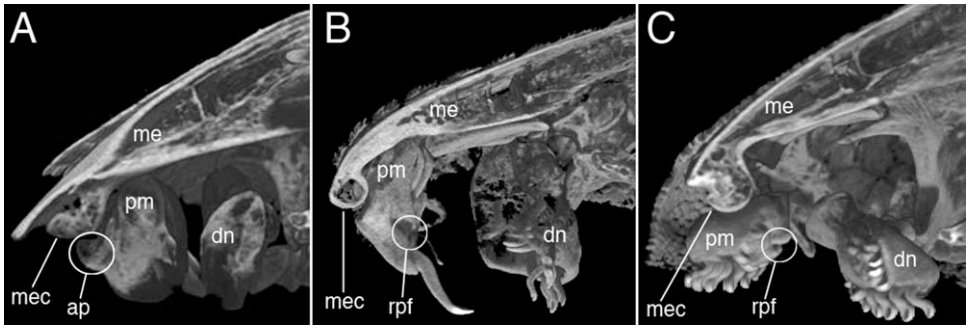

Fig. 2. Computed tomography images of the medial and sagittal sections through the snout and mouth of three species representative of jaw morphological diversity across the Loricariidae: **A**: *Chaetostoma* cf. *milesi*, **B**: *Leporacanthicus joselimai*, and **C**: *Panaque nigrolineatus*. Labels: ap, ascending process of the premaxilla, dn, dentary; me, mesethmoid; mec, mesethmoid condyle; pm, premaxilla; rpf, retractor premaxillae fossa. Digital sectioning was made from CT data using the VG Studio Max software package.

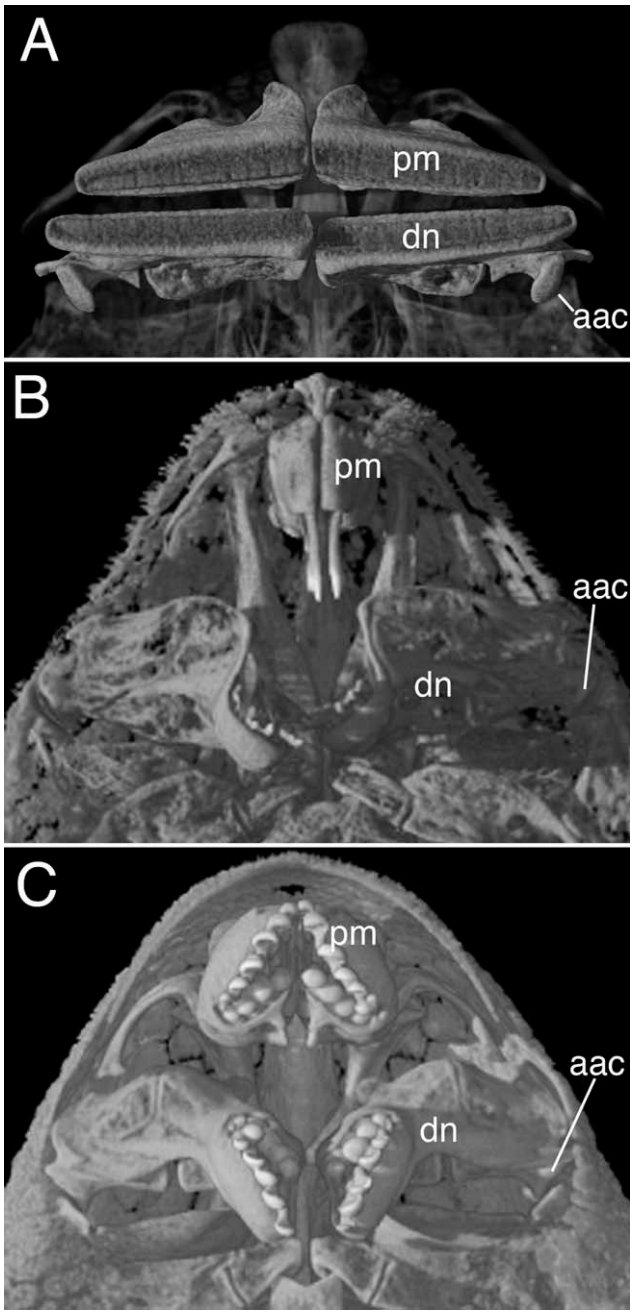

Fig. 3. Computed tomography images of the ventral views of the snout and mouth of three species representative of jaw morphological diversity across the Loricariidae: **A**: *Chaetostoma* cf. *milesi*, **B**: *Leporacanthicus joselimai*, and **C**: *Panaque nigrolineatus*. Labels: dn, dentary; pm, premaxillae; aac, anguloarticular condyle.

iid lower jaw is mainly in the sagittal plane around a transverse axis like most other vertebrates. However, Loricariidae differ from most other vertebrates by having mandibles that extend medially from a lateral condyle and that lack a medial stabilizing connection to the opposite ramus (Fig. 3), permitting limited additional rotational freedom in horizontal and vertical planes. In most vertebrates, the medial mandibular symphysis restricts lower jaw rotation to the sagittal plane. The absence of this and other key biomechanical linkages in loricariids appears to allow three-dimensional freedom of independent upper and lower jaw movement that is unparalleled among fishes (Adriaens et al., 2009).

Loricariid jaws are specialized for constant or periodic contact with variable, uneven substrates throughout adduction, and rotational kinematics likely vary in response to substrate heterogeneity. Given this high degree of kinetic freedom, the scarcity of empirical kinetic data, and the potential for interspecific variation in mandibular kinetics, any advancement of a generalized model of loricariid lower jaw function must be done cautiously but with the goal of generating specific functional hypotheses that are experimentally testable. Our goals in this study are 1) to identify several discrete, interspecifically comparable, and functionally relevant aspects of loricariid jaw morphology, 2) to measure these aspects across a taxonomically broad range of loricariids, 3) to examine patterns among phylogenetically diagnosed taxa in an evolutionary context, and 4) to combine these data with available kinetic data to make explicit predictions about how interspecific morphological variation might be linked to functional diversity across the family.

MATERIALS AND METHODS

Specimen Collection and Preparation

Twenty-five species from two subfamilies within Loricariidae were examined (2–83 specimens per species; 377 specimens total; Table 1). All specimens were collected in August 2006 by seining and electrofishing middle reaches of the Marañon River, a tributary of the upper Amazon River in northern Peru. Most sampled species (n = 20) belonged to subfamily Hypostominae; within this subfamily, most (n = 16) belonged to tribe Ancistrini. Other species belonged to the Hypostominae, Hypostomini (n = 4 spp.); Loricariinae, Harttiini (n = 3 spp.); and Loricariinae, Loricariini (n = 2 spp.). "New Genus" refers to New Genus 3 in Armbruster (2008), an undescribed genus and species of Ancistrini (Hypostominae). Taxonomic delineations follow the phylogenetic studies of Armbruster (2004, 2008) and Rapp Py-Daniel (1997), which diagnose subfamilies, tribes, and many of the genera discussed herein using largely nonmandibular morphological synapomorphies. No phylogenies currently exist that incorporate all species in this study.

Functional examination and homologous comparison of loricariid premaxillae are complicated by their extreme reduction or near-absence in some taxa (e.g., *Reganella* and *Pseudohemiodon*; Rapp Py-Daniel, 1997) and by their loose suspension via a highly variable cartilaginous meniscus in all taxa. For this study, we examined the right mandible, which was dissected from each specimen and individually cleared and stained (Fig. 4). Loricariid mandibles examined in this study were small, ranging from 3 to 15 mm in greatest dimension. To facilitate their manipulation and imaging, all soft tissue was removed following clearing and staining and ossified elements were allowed to air dry. All dissections were made from voucher specimens cataloged at the Auburn University Museum Fish Collection, Auburn, Alabama.

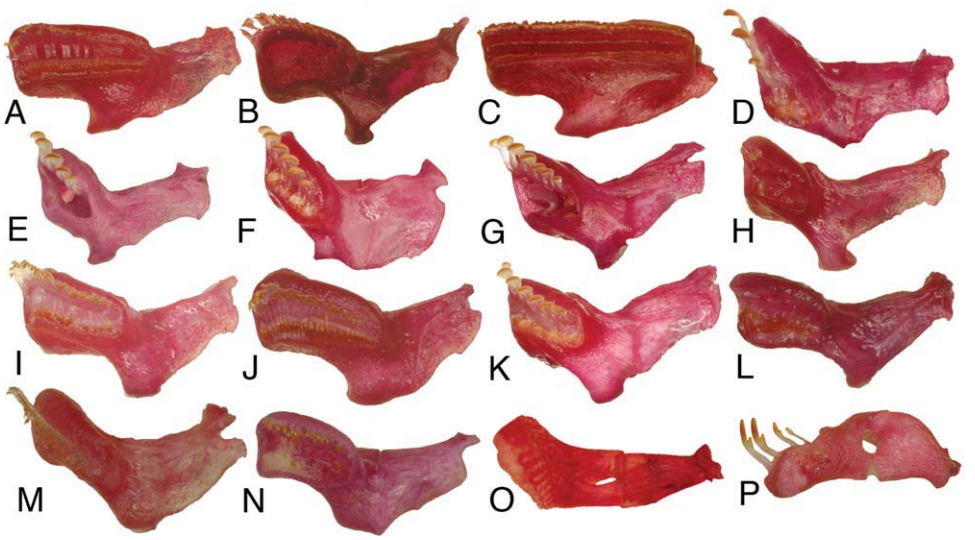

Fig. 4. Representative sample of lower jaws from Loricariidae examined in this study: Hypostominae: Ancistrini: **A**: *Ancistrus* sp. "longjaw," **B**: *Ancistrus* sp. "shortjaw," **C**: *Chaetostoma* sp. 1, **D**: *Panaque albomaculatus*, **E**: *Panaque gnomus*, **F**: *Panaque* cf. *bathyphilus*, **G**: *Panaque nocturnus*, **H**: *Peckoltia bachi*; Hypostominae: Hypostomini: **I**: *Hypostomus emarginatus*, **J**: *Hypostomus niceforoi*, **K**: *Hypostomus pyrineusi* (*H. cochliodon* group), **L**: *Hypostomus unicolor*; Loricariinae: Harttiini: **M**: *Farlowella amazonum*, **N**: *Lamontichthys filamentosus*, **O**: *Rineloricaria lanceolata*; Loricariinae: Loricariini: **P**: *Spatuloricaria puganensis*. [Color figure can be viewed in the online issue, which is available at wileyonlinelibrary.com.]

Digital images were captured of each lower jaw element in at least two orthogonal perspectives of the three illustrated in Figure 5 using a Nikon Coolpix 990 digital camera mounted to a Leica MZ6 stereomicroscope. Twisting along the long axis of the lower jaw and major evolutionary shifts in the relative position and orientation of distal versus proximal jaw regions preclude the designation of homologous perspectives from which all jaw regions could be imaged in a standardized manner. Jaw orientations were therefore arbitrarily standardized using the broad anguloarticular-dentary coronoid flange as a reference, ensuring that this flange was either parallel or perpendicular to the field of view. Horizontal orientations in vertical (Fig. 5A,D) and dorsal (Fig. 5C,F) perspectives were defined as having the flange parallel with the stage, and vertical orientations (Fig. 5B,E) were defined as having the flange perpendicular to the stage. These positions were also stable resting positions for many mandibles, and they presented at least one and often two parameters in parallel with and proximal to the stage, minimizing potential error from parallax. Wire mesh was used as a support for specimens that were unstable in a given orientation. Length and area measurements were made digitally using tpsDIG2 software (Rohlf, 2008, v. 2.12) and were individually standardized to a scale bar visible in each frame.

To maximize the functional and anatomical homology of our measurements and minimize the ramifications of tooth loss during clearing and staining and soft tissue removal, parameters defined as distances to or between teeth were measured to tooth insertions rather than tooth cusps, and dentition was not explicitly examined. Loricariidae exhibit considerable variation in tooth number, morphology, length, rigidity, and cusp dimensions (e.g., Fig. 3; Muller and Weber, 1992; Delariva and Agostinho, 2001; Geerinckx et al., 2007b), each of which has potential functional ramifications that remain to be investigated. We excluded such variation but acknowledge its importance and hope that our results might spur its future study.

Computer-Aided Tomography Data

Single specimens of three loricariid species (*Chaetostoma* cf. *milesi*, *Panaque nigrolineatus*, and *Leporacanthicus joselimai*) selected to represent jaw diversity across the Loricariidae were sent to the Digimorph High-Resolution X-ray Computer-Aided

TABLE 1. Species, taxonomic rank affiliations, sample sizes, and angular mean of the tooth row angle (TR_{angle}) for individuals examined herein

Species	N jaw	N AM_{vol}	Mean TR_{angle}
Subfamily: Hypostominae			
Tribe: Ancistrini			
Ancistrus sp. "longjaw"	5		8°
Ancistrus sp. "shortjaw"	3		11°
Ancistrus sp. "wormline"	2		13°
Chaetostoma lineopunctatum	4		19°
Chaetostoma microps	27*	6	18°
Chaetostoma sp. 1	27*		20°
Chaetostoma sp. 2	16*	6	16°
Chaetostoma sp. 3	33*	6	18°
Chaetostoma sp. 4	15*		19°
Lasiancistrus schomburgkii	22*	6	20°
New Genus	18*	6	21°
Panaque albomaculatus	13*	4	51°
Panaque gnomus	30*	6	38°
Panaque cf. *bathyphilus*	13*	5	32°
Panaque nocturnus	83*	6	30°
Peckoltia bachi	2		26°
Tribe: Hypostomini			
Hypostomus emarginatus	3		21°
Hypostomus niceforoi	4		21°
Hypostomus pyrineusi	19*	6	27°
Hypostomus unicolor	4		22°
Subfamily: Loricariinae			
Tribe: Farlowellini			
Farlowella amazonum	3		31°
Tribe: Harttiini			
Lamontichthys filamentosus	18*	6	16°
Tribe: Loricariini			
Loricaria clavipinna	3		36°
Rineloricaria lanceolata	3		50°
Spatuloricaria puganensis	9*	4	38°

Asterisks indicate that allometric scaling was examined. All specimens were collected from middle reaches of the Marañon River, a tributary of the upper Amazon in northern Peru.

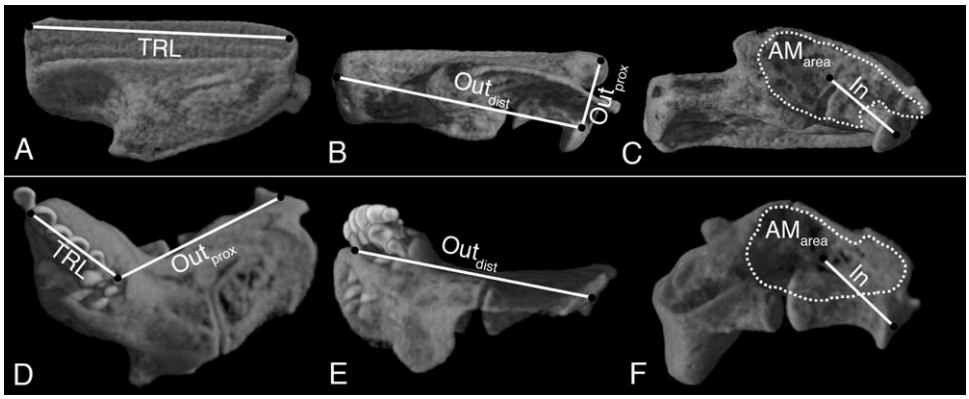

Fig. 5. Computed tomography images of the lower jaw ramus of *Chaetostoma* cf. *milesi* (**A–C**) and *Panaque nigrolineatus* (**D–F**) rotated to illustrate the horizontal orientation, ventral perspective (A, D), vertical orientation (B, E), and horizontal orientation, dorsal perspective (C, F). Parameters measured herein are labeled according to the perspective and view from which they were measured: AM_{area}, adductor mandibulae insertion area; In, in-lever from center of adductor mandibulae area of insertion to angularticular condyle; Out_{dist}, out-lever from anguloarticular condyle to distalmost tooth; Out_{prox}, out-lever from angularticular condyle to proximalmost tooth; TRL, tooth row length.

Tomography (CT) Facility at the University of Texas, Austin. CT data were edited, and images for Figs. 2, 3, 5, and 6 were generated using the VG Studio Max software package at the Academy of Natural Sciences, Philadelphia.

Morphometrics

We quantified variation in shape of the mandible using a largely one-dimensional approach that minimizes error from variation in perspective and focuses on functional relevance. Five linear distances and one area (hereafter referred to as parameters) were measured from digital images of each mandible (Fig. 5). Three of the five linear distance parameters were analogous with input and output lever arms for mandibular adduction in the majority of Actinopterygii (Westneat, 2004), providing continuity with previous investigations of fish jaw mechanics. These linear distances were measured from a midpoint along the surface of the anguloarticular condyle (AAC) to respective distalmost (Out_{dist}; Fig. 5B,E) and proximalmost (Out_{prox}; Fig. 5B,D) tooth insertions and from a midpoint along the AAC surface to the center of the adductor mandibulae insertion area (In; Fig. 5C,F).

To quantify morphological and functional variation specific to the Loricariidae, three parameters (two linear distance parameters and one area parameter) not typically examined in other fish jaw studies were also measured. First, distance from proximalmost to distalmost tooth insertions (tooth row length, TRL; Fig. 5A,D) was measured and treated as the distance across which force transmitted through the mandible may be distributed to the substrate. A distance perpendicular to the line between the AAC and the distalmost tooth (Out_{dist}) and from that line to the apex of the coronoid arch was also measured (H1; Fig. 6). H1 quantified variation in the height or maximum excursion of the coronoid arch relative to the distalmost tooth. This parameter describes morphological variation that we hypothesize is a central means by which torque into the mandibule changes across the family.

Finally, we measured the area of a distinct, shallowly concave region on the posterodorsal surface of the anguloarticular-dentary coronoid flange in which the largely columnar adductor mandibulae muscle inserts broadly (AM_{area}; Fig. 5C,F). Among a subset of 12 species (Table 1), AM_{area} correlated with AM volume (AM_{vol}; Fig. 7; $R^2 = 0.69$, $P < 0.001$), suggesting that this parameter provides a reliable predictor of interspecific variation in maximum force applicable to the mandible. We examined the relationship between AM_{area} and AM_{vol} by removing the left combined AM (A1-OST and A3′ divisions; Geerinckx, 2006) and measuring its volume by displacement. Because AM_{area} and AM_{vol} data were collected from separate specimens at separate times, each was standardized to the respective square and cube

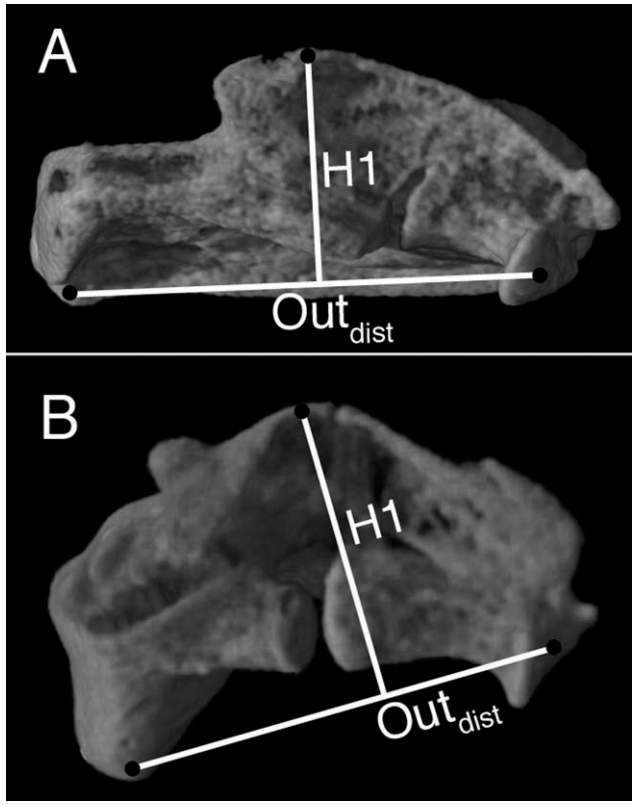

Fig. 6. Computed tomography images of the lower jaw ramus of **A**: *Chaetostoma* cf. *milesi* and **B**: *Panaque nigrolineatus* in horizontal orientation, dorsal perspective to illustrate distances defined as the distalmost out-lever (Out_{dist}) and coronoid height (H1) parameters.

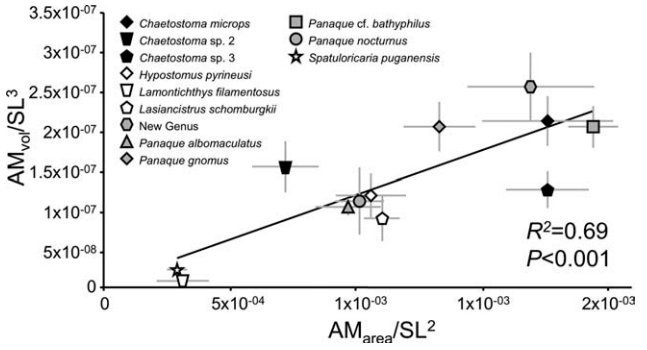

Fig. 7. Relationship between combined adductor mandibulae area of insertion (AM_{area}) scaled to the square of standard length (SL) and adductor mandibulae volume (AM_{vol}) scaled to SL^3. AM_{area} and AM_{vol} were measured from separate specimens, so the interspecific correlation was derived from the mean values for each species. Plotted values are means ± standard deviation. See Table 1 for species sample sizes.

of specimen standard length (SL). Interspecific variation was then investigated via regression of mean AM_{vol}/SL^3 against mean AM_{area}/SL^2 (Fig. 7).

Allometric Scaling

Allometric scaling was examined in a subset of 14 species for which sample sizes allowed statistical comparison (Table 1). The five linear parameters defined above, plus the square root of the AM_{area} parameter, were each divided by standard body length (SL), and orthogonal variation among these standardized data was ordinated using a principal component (PC) analysis of covariance. To test for systematic allometric variation, the first four PCs were regressed against SL.

Phylogenetic Patterns of Mandibular Diversity

To examine orthogonal patterns of interspecific morphological variation, we conducted a PC analysis of the entire data set of six parameters × 377 individuals. The color of individual markers was then varied to illustrate the distributions in mandibular morphospace of various taxonomic groupings that corresponded with successively nested, phylogenetically diagnosed clades (Rapp Py-Daniel, 1997; Armbruster, 2004, 2008).

Functional Hypotheses

Select parameters were related to each other as a series of six putatively functionally significant metrics: two traditional ratios of mechanical advantage (MA), three novel ratios, and one angle. The first novel ratio, AM_{area}/TRL^2, is distinguished from all other metrics by allowing functional interpretation without reference to the complex geometry and variable kinetics of loricariid mandibles. The other five metrics describe variation in geometric relationships among areas of force-in and force-out, indicating their relevance to predictions of MA:

- In/Out_{dist}: traditional calculation of MA at distalmost tooth.
- In/Out_{prox}: traditional calculation of MA at proximalmost tooth.
- H1/TRL: interpreted as a combined measure of torque and the distance across which force transmitted through the mandible can be instantaneously delivered to substrates.
- Out_{dist}/H1: a ratio of the major length vs. height dimensions of the mandible; interpreted as a measure of the predominant plane (sagittal vs. horizontal) of torque through the lower jaw.
- TR_{angle} (calculated trigonometrically by treating Out_{dist}, Out_{prox}, and TRL as sides of a scalene triangle): interpreted as a measure of the maximum excursion of the distalmost tooth and as a novel, more reliable indicator of variation in torque output from the mandible than the traditional parameters defined above. The externally visible angle between left and right mandibular tooth rows (the intermandibular tooth row angle; Figs. 1 and 3) is a taxonomically important, interspecifically variable character used to diagnose several loricariid genera and species. *Peckoltia* and *Hemiancistrus*, for example, are currently differentiated solely on whether intermandibular tooth row angle is $<90^\circ$ (*Peckoltia*) or $>100^\circ$ (*Hemiancistrus*; Armbruster, 2008). TR_{angle} values reported here are inversely proportional to intermandibular tooth row angles reported in other studies.

MA is the factor by which a rotating system, or lever, multiplies force; it can be predicted by dividing the in-lever by the out-lever, with high values indicating greater transmission of force and low values indicating faster rotation. Fish jaw in-levers are commonly defined as distances from the AAC to the center of the area of adductor mandibulae insertion, and out-levers as distances from the AAC to points of force-out (typically tooth cusps; Westneat, 2004). We calculated two relatively traditional metrics of jaw closing MA (In/Out_{dist} and In/Out_{prox}) and used a 3D rotating cone model of loricariid lower jaw function (Fig. 8) to illustrate potential problems with applying traditional MA metrics to loricariid jaws and to develop novel functional hypotheses specifically relevant to the loricariid jaw.

Rotating Cone Model

This mechanical model (Fig. 8) examines geometric and functional relationships between the parameters defined above and known axes of mandibular rotation (Adriaens et al., 2009). The model allows the functional relevance of each parameter to be examined individually and in combination with other parameters and provides a theoretical framework in which traditional versus novel functional metrics may be evaluated.

Loricariid mandibles differ from most other vertebrate mandibles by being transversely oriented and elongated along their primary axis of rotation (Fig. 8, Axis 1). In contrast, most other vertebrate mandibles are sagittal in orientation and largely perpendicular to their primary axis of rotation. Although both a generalized loricariid mandible and a generalized vertebrate mandible rotate primarily within the sagittal plane (around a transverse axis; Fig. 8, Axis 1), only the generalized vertebrate mandible is elongated and flattened with respect to the sagittal plane. Most vertebrate mandibles may therefore by modeled as a body rotating in two dimensions (Westneat, 2003, 2004). Given the $\sim 90^\circ$ shift in orientation of the loricariid mandible, three dimensions must be taken into consideration, and the relative position and orientation of lever arms that control mandibular MA must be reevaluated.

Traditional metrics of fish jaw MA are likely inadequate for understanding loricariid mandibular function because the anatomical dimensions used to define these lever arms (e.g., distance between the AAC and distalmost tooth) have shifted with mandibular evolution so that they are oriented approximately perpendicular to the sagittal plane of rotation and are nearly parallel with the transverse axis of rotation (Fig. 8, Axis 1). Only the component of a given lever that is perpendicular to the rotational axis actually controls MA of a rotating body. To evaluate novel lever arm dimensions that might provide a more accurate estimate of MA than traditionally defined lever arms, we relate the measured parameters to each other in the framework of a rotating cone (Fig. 8).

A central component of the rotating cone model is the output triangle with sides formed by the traditionally defined output lever arms (Out_{prox}, Out_{dist}) and the tooth row (TRL; output tri-

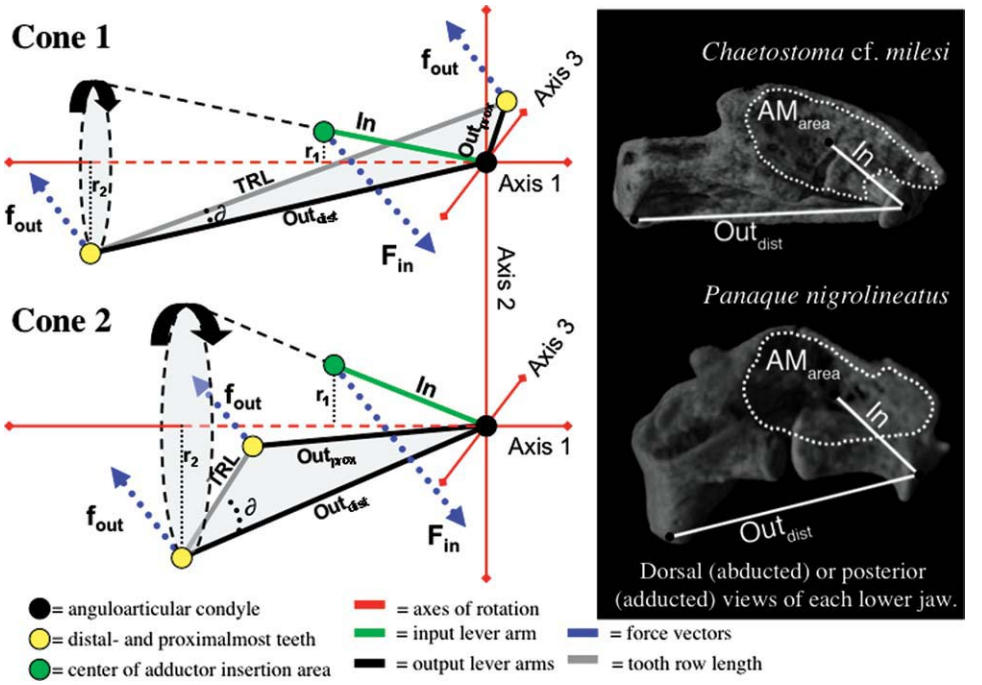

Fig. 8. Three-dimensional rotating cone model linking parameters measured herein to a hypothesis of jaw kinesis. Upper and lower cones are modeled after the right lower jaw ramus of *Chaetostoma* cf. *milesi* (Cone 1) and *Panaque nigrolineatus* (Cone 2), which illustrate near opposite ends of a spectrum of mandibular parameters discussed in this study. Perspective is a dorsal view of an abducted mandible or posterior view of an adducted mandible. Red lines are potential axes of rotation, with Axis 1 representing rotation in the sagittal plane, Axis 2 representing rotation in the horizontal plane, and Axis 3 representing rotation in the transverse plane. Capitalized parameters and parameters represented by solid green, black, and gray lines were measured or quantified by proxy in this study (Fig. 5). See text for discussion of output triangle (gray triangle). Tooth row angle (TR_{angle}) is indicated by ∂.

angle shaded gray, Fig. 8). The posterolateralmost vertex of the output triangle is the AAC—the fulcrum for mandibular rotation. The remaining vertices are the distalmost and proximalmost tooth insertions (yellow circles, Fig. 8), which delimit the region across which mandibular force is distributed to substrates. Extending dorsomedially away from the AAC, oblique with respect to the output triangle, is the traditionally defined in-lever arm (In, Fig. 8).

Interpretation and discussion of the rotating cone model are largely contingent upon four assumptions, the first three of which are supported by kinematic data from a single species (Adriaens et al., 2009): 1) rotation is predominantly in the sagittal plane (around Axis 1; Fig. 8), 2) rotation in the horizontal plane (around Axis 2; Fig. 8) is secondary, and 3) rotation in the transverse plane (Axis 3; Fig. 8) is negligible. The fourth assumption is that the predominant rotational axis (Axis 1) crosses through a midpoint along the transverse axis of the ramus, approximately equidistant from the input lever arm and the output triangle.

To simplify loricariid mandibular mechanics, the cone models (Fig. 8) focus on dimensions that are most relevant to MA at the distalmost tooth. Excursion of the distalmost tooth during adduction can be visualized as an arc traced around the base of the cone. Functionally important aspects of interspecific morphological variation can be represented by cones of different dimensions: 1) a relatively long cone with a small base, a small angle between in-lever and output triangle, and lesser excursion of the distalmost tooth (Fig. 8: Cone 1, e.g., *Chaetostoma* cf. *milesi*), and 2) a shorter cone with a larger base, a greater angle between in-lever and output triangle, and greater excursion of the distalmost tooth (Fig. 8: Cone 2, e.g., *Panaque nigrolineatus*). Interspecific variation in TRL and tooth row angle (TR_{angle}, ∂) are also illustrated, with Cone 1 having a relatively long tooth row and a small tooth row angle, and Cone 2 having a shorter tooth row and a greater tooth row angle.

The geometry and mechanics of these models indicate that MA at the distalmost tooth may be most accurately predicted by treating the parameter r_1 as an input lever and parameter r_2 as an output lever. Parameter r_1 is the shortest distance from the center of adductor mandibular insertion to the transverse axis of rotation (Axis 1), and r_2 is the shortest distance from this axis to the distalmost tooth. Although we could not measure these parameters, we suggest below that r_1 likely covaries in relation to the parameter H1, and r_2 likely covaries in relation to TR_{angle}.

RESULTS

Allometric Scaling

Species-specific PC analyses of mandibular parameters standardized to SL revealed systematic, allometric variation in aspects of mandibular shape that varied within and among genera (Table 2). Regression of PCs 1–4 against SL revealed significant correlation between mandibular shape and body size in 10 of the 14 species examined, but there was no clear pattern across these 10 species. Species with allometric variation differed in both the strength of allometry (R^2 and % variance explained by allometric PCs) and in the parameters that appeared to be main sources of the effect (as inferred from PC loading scores). The parame-

TABLE 2. First four principal components (PCs) and the % variance (% var) they explain, from a PC analysis of mandibular parameters standardized to standard length

Species	PC1			PC2			PC3			PC4			Highest loading parameters*
	% var	R^2	*P*	% var	R^2	*P*	% var	R^2	*P*	% var	R^2	*P*	
Chaetostoma microps	71	0.01	0.614	**12**	**0.16**	**0.039**	8	0.07	0.189	**5**	**0.24**	**0.010**	H1, In
Chaetostoma sp. 1	**90**	**0.46**	**0.003**	5	0.12	0.179	2	0.13	0.150	1	0.04	0.436	Out_{dist}
Chaetostoma sp. 2	66	0.10	0.227	14	0.00	0.853	9	0.01	0.731	**3**	**0.21**	**0.074**	In
Chaetostoma sp. 3	**60**	**0.23**	**0.005**	**18**	**0.38**	**0.000**	10	0.00	0.702	6	0.00	0.939	TRL, H1
Chaetostoma sp. 4	62	0.18	0.117	18	0.00	0.812	9	0.14	0.167	7	0.01	0.710	TRL
Hypostomus pyrineusi	**58**	**0.38**	**0.005**	23	0.00	0.911	**9**	**0.23**	**0.037**	6	0.04	0.399	Out_{dist}, H1
Lamontichthys filamentosus	**96**	**0.48**	**0.002**	2	0.08	0.244	1	0.09	0.222	1	0.01	0.646	Out_{dist}
Lasiancistrus schomburgkii	67	0.03	0.405	**18**	**0.29**	**0.010**	7	0.01	0.624	4	0.07	0.237	TRL
New Genus	**50**	**0.22**	**0.052**	27	0.06	0.340	**13**	**0.21**	**0.053**	7	0.12	0.152	TRL, Area
Panaque albomaculatus	60	0.09	0.311	26	0.14	0.214	7	0.01	0.776	**5**	**0.37**	**0.027**	Out_{prox}
Panaque cf. *bathyphilus*	50	0.27	0.105	36	0.07	0.423	8	0.16	0.219	3	0.01	0.806	–
Panaque gnomus	71	0.02	0.484	10	0.02	0.410	**9**	**0.11**	**0.075**	**5**	**0.15**	**0.034**	Out_{dist}, Out_{prox}
Panaque nocturnus	**65**	**0.15**	**0.000**	14	0.00	0.700	**9**	**0.11**	**0.003**	6	0.02	0.230	Out_{dist}, H1
Spatuloricaria puganensis	**76**	**0.45**	**0.049**	17	0.00	0.886	6	0.16	0.294	1	0.08	0.457	Out_{prox}

R^2 and *P* values describe the relationship of each principle component to species standard length. PCs that are significantly related to SL ($P < 0.1$) are in boldface. Highest loading parameters are those parameters with the highest magnitude eigenvectors for those PCs with allometric variation (*).

ter most commonly recovered as highest loading on allometric PCs was Out_{dist} ($n = 5$ spp.), followed by H1 ($n = 4$ spp.) and TRL ($n = 4$ spp.; Table 2).

Taxonomic Partitioning of Mandibular Morphospace

PC analysis of mandibular morphometrics described broad conservatism and overlap at the taxonomic ranks of subfamily and tribe, and dispersion and mutual exclusion at the ranks of genus and species (Fig. 9). Subfamily Hypostominae (including tribes Ancistrini and Hypostomini) and subfamily Loricariinae (including tribes Loricariini, Farlowellini, and Harttiini) broadly overlap in mandibular morphospace as described by PCs 1–4 (Fig. 9A,B). Groupings within each subfamily also occupied unique, nonoverlapping regions of morphospace, and these groupings mostly comprised nested clades coinciding with less inclusive taxa. Within subfamily Hypostominae, mandibular morphospace of the genus-poor tribe Hypostomini was largely encompassed within the broad distribution of the genus-rich tribe Ancistrini (Fig. 9A,B). Ancistrini exhibited the broadest range of mandibular morphospace, but was also represented by the greatest taxonomic diversity and largest sample size in the data set.

Mandibular morphologies of ancistrine genera *Ancistrus, Chaetostoma*, *Lasiancistrus, Panaque*, and New Genus exhibited largely nonoverlapping distributions along PC2 (Fig. 9C), whereas the ancistrine genus *Peckoltia* (represented here by 2 individuals; Table 1) was nested largely within the distribution of *Panaque* (Fig. 9C). The ancistrine genus *Chaetostoma* occupied a unique region of mandibular morphospace along the PC2 axis (Fig. 9C), and six *Chaetostoma* species partially segregated this space along a continuum described by PCs 1 and 2 (Fig. 9E). Four species in the ancistrine genus *Panaque* exhibited a largely nonoverlapping distribution within mandibular morphospace described by PCs 3 and 4 (Fig. 9F). Of these, three species overlapped broadly with other loricariid species, whereas *Panaque* cf. *bathyphilus* occupied a unique region of mandibular morphospace along the PC3 axis (Fig. 9F). Of four species in the hypostomine genus *Hypostomus*, all clustered together on PC 3 and 4 axes (not illustrated), and three (*H. niceforoi, H. unicolor*, and *H. emarginatus*) clustered together along the PC2 axis (Fig. 9G), whereas *H. pyrineusi* formed a distinct group largely overlapping the distribution of the ancistrine genus *Panaque* (Fig. 9C,G). In contrast to the other *Hypostomus* species examined herein, *H. pyrineusi* is known to specialize on a diet of wood, as do all members of the ancistrine genus *Panaque*.

Within subfamily Loricariinae, tribe Loricariini occupied a unique region of morphospace as described by PC 4 (Fig. 9B,D), whereas Farlowellini and Harttiini were largely indistinguishable from members of the Hypostominae across PCs 1–4 (Fig. 9A,B). Mandibular morphospace occupied by Loricariini appears to be partially segregated by the three loricariine genera examined herein (Fig. 9D), although sample sizes of the genera *Loricaria* and *Rineloricaria* were too small to draw strong conclusions.

Functional Ratios: Force Intensity

The ratio AM_{area}/TRL^2 was calculated as a predictor of maximum force entering the mandible per unit of substrate contacted. This ratio produced a range of mean values (Fig. 10 and Supporting Information Fig. S1) from 0.14 for *Chaetostoma* sp. 2 to 2.03 for *Peckoltia bachi*. *Chaetostoma* spp. were clustered at the low end of the range,

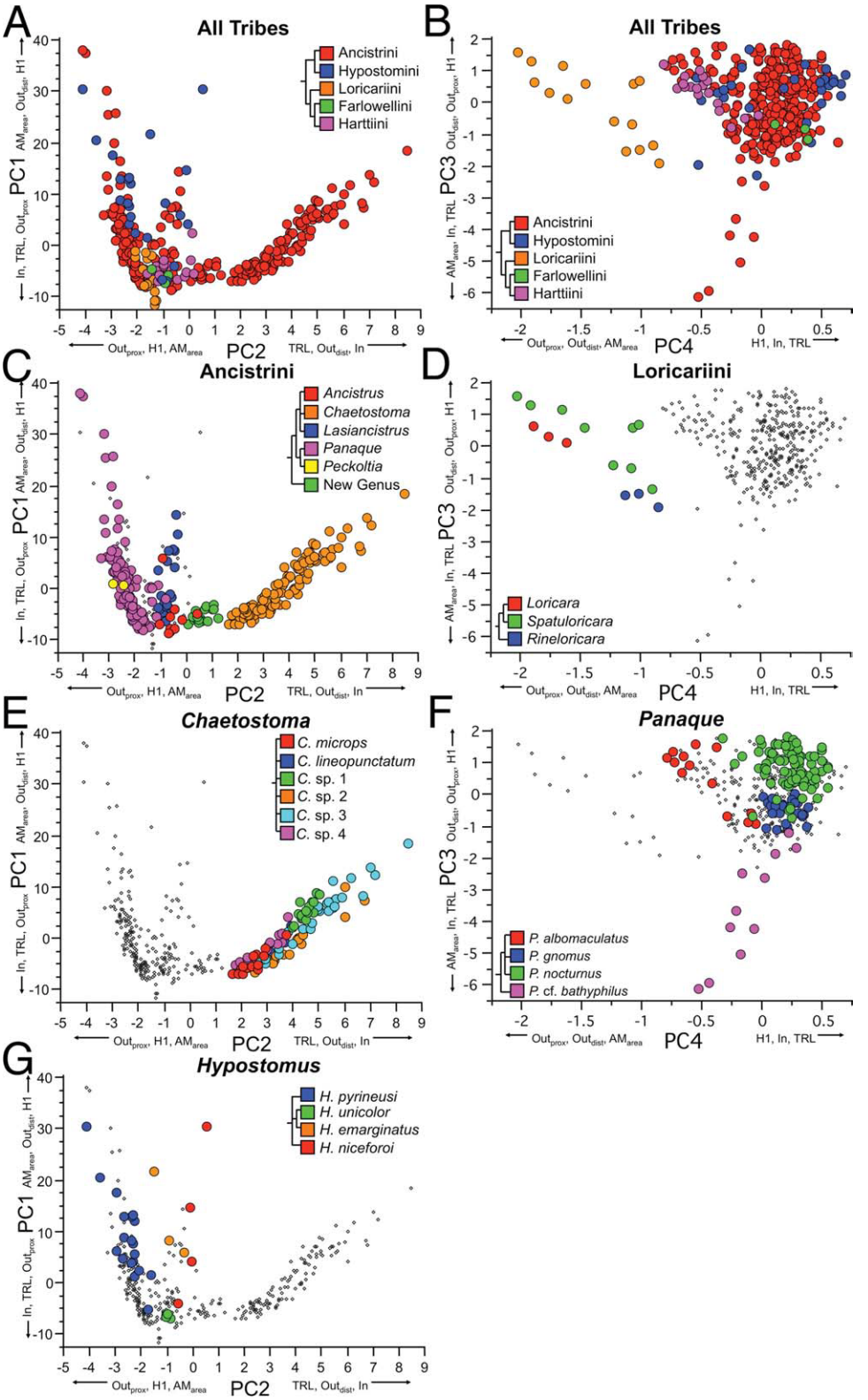

Fig. 9. Principal component (PC) analysis of six morphometric parameters hypothesized to be functionally relevant to the loricariid lower jaw (illustrated in Figs. 5 and 6). Analysis included 377 individuals and 25 species of Loricariidae collected in the upper Amazon Basin of northern Peru (Table 1). Parameters listed along each PC axis in order of their eigenvector, with arrows indicating direction of influence (Table 3). Illustrated phylogenetic relationships follow Armbruster (2008), Rapp Py-Daniel (1997), and Sullivan et al. (2006).

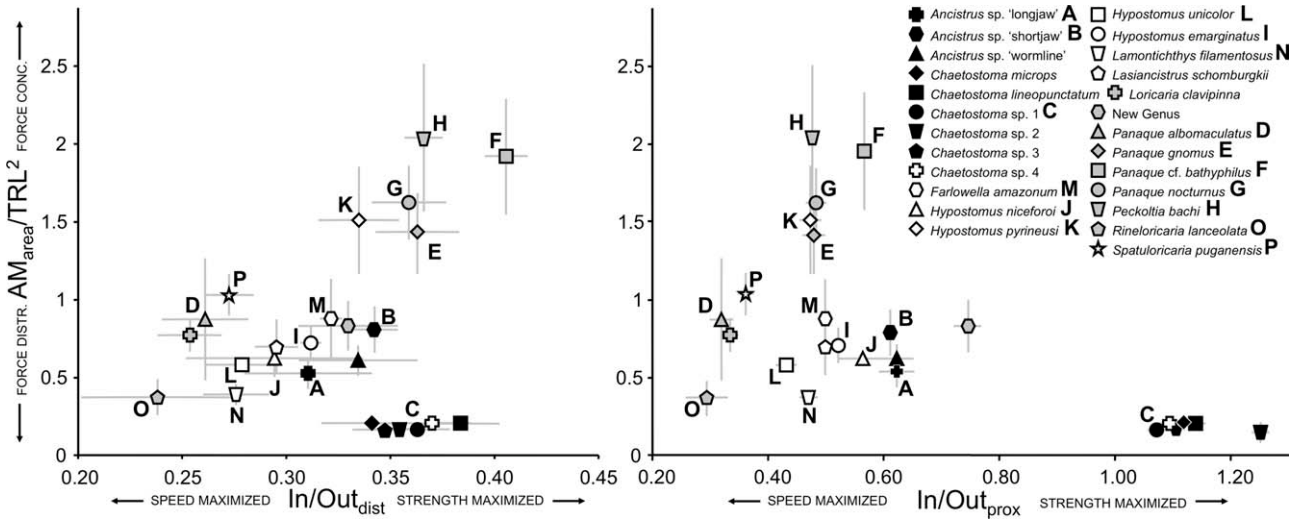

Fig. 10. The novel metric of force intensity AM_{area}/TRL^2 plotted against traditional metrics of mechanical advantage: distance from anguloarticular condyle to center of adductor mandibulae insertion area (In) over respective distances from anguloarticular condyle to distalmost (Out_{dist}) and proximalmost (Out_{prox}) tooth insertions. Capital letters refer to jaws illustrated in Figure 4. Plotted values are means ± standard deviation. Sample sizes are given in Table 1.

with mean values from 0.15 to 0.21, whereas the middle range from about 0.37 to 1.03 included several genera from both subfamilies Hypostominae and Loricariinae. Values from 1.43 and up included only *Peckoltia bachi* (Ancistrini) and the wood-eating species *Hypostomus pyrineusi* (Hypostomini) and *Panaque* spp. (Ancistrini).

Functional Ratios: Jaw Geometry and Traditional Metrics

Two linear distance ratios, In/Out_{dist} and In/Out_{prox}, were computed as predictions of mandibular MA largely consistent with previous investigations of teleost jaw function. In/Out_{dist}, or putative MA to the distalmost tooth, ranged from 0.24 for *Rineloricaria lanceolata* to 0.41 for *Panaque* cf. *bathyphilus* (Fig. 10). All other species were distributed continuously between 0.26 (*Panaque albomaculatus*) and 0.38 (*Chaetostoma lineopunctatum*). In/Out_{prox}, or putative MA to the proximalmost tooth, ranged from a low of 0.30 for *Rineloricaria lanceolata* to 1.26 for *Chaetostoma* sp. 2 (Fig. 12). Three Loricariini species (*Loricaria clavipinna*, *Rineloricaria lanceolata*, and *Spatuloricaria puganensis*) and one Ancistrini species (*Panaque albomaculatus*) clustered at the low end below 0.40, and *Chaetostoma* species clustered at the high end above 1.08. All other species were distributed more or less continuously between 0.44 and 0.75 (Fig. 10).

Functional Ratios: Jaw Geometry and Novel Metrics

Two linear distance ratios (H1/TRL, Out_{dist}/H1) and one angle (TR_{angle}) were computed as novel metrics with putative relevance to the highly specialized form and function of the loricariid mandible. H1/TRL is hypothesized to be a combined measure of MA and force intensity. Values of H1/TRL (Fig. 11) ranged from a low-end cluster of *Chaetostoma* species (0.44–0.50) plus *Rineloricaria lanceolata* (0.63) to a high-end cluster of the *Panaque* species *P. gnomus, P. nocturnus*, and *P.* cf. *bathyphilus* (1.6–1.9) plus *Peckoltia bachi* (2.1; all Ancistrini) and *Hypostomus pyrineusi* (1.8; Hypostomini). All other species were distributed more or less continuously between 0.7 (*Loricaria clavipinna* and New Genus) and 1.3 (*Farlowella amazonum*).

Out_{dist}/H1, which relates a mandibular length dimension (Out_{dist}) to a mandibular height dimension (H1), is hypothesized to be an indicator of the mandibular plane in which the greatest torque is experienced, with lower values suggesting greater torque in the sagittal plane and higher values suggesting greater torque in the horizontal plane (Fig. 11). This metric is based on the principle that in any rotating system, torque is greatest at the point furthest from the axis of rotation. A mandible that is more transversely elongate with teeth far from the axis of rotation (e.g., Fig. 3: O, P) will likely experience more torque in the horizontal plane, whereas mandibles that are more transversely compressed and have high TR_{angle} and a tall coronoid arch (H1; e.g., Fig. 3E,F) will likely experience more torque in the sagittal plane. Most species were distributed continuously from ~1.6 (*Farlowella amazonum, Panaque gnomus, P. nocturnus*, and *P.* cf. *bathyphilus*) to 2.4 (*Chaetostoma microps*), but much higher values were obtained for the Loricariini species *Spatuloricaria puganensis* (2.8), *Rineloricaria lanceolata* (3.7), and *Loricaria clavipinna* (3.9).

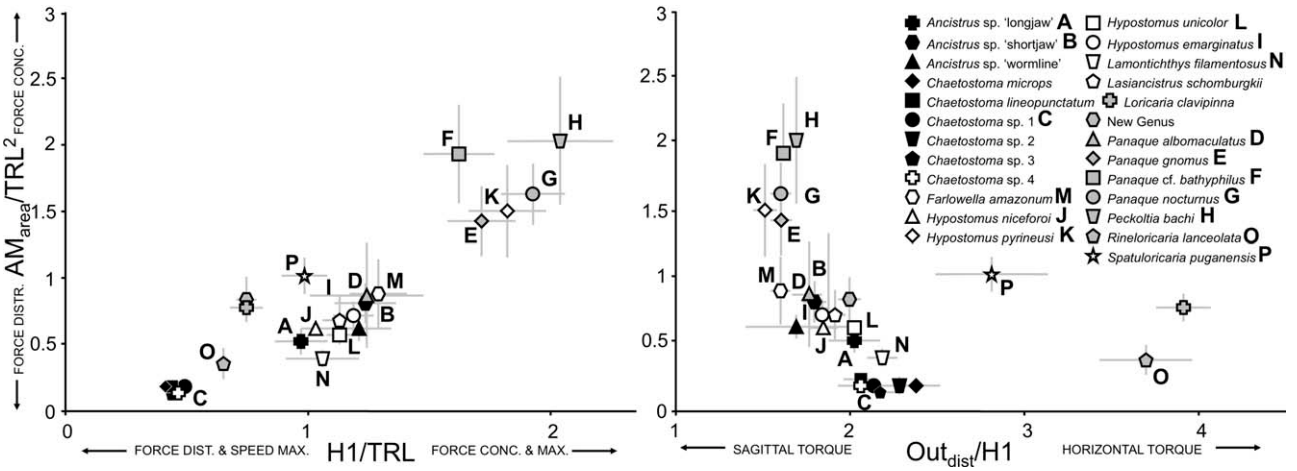

Fig. 11. The novel metric of force intensity AM_{area}/TRL^2 plotted against two other novel metrics of lower jaw function: The distance parameter H1 (Fig. 6) over TRL, interpreted as a combined measure of torque magnitude entering the mandibular lever and the distance across which force transmitted through the mandible can be instantaneously delivered to substrates, and the distal out-lever arm (Out_{dist}, Fig. 5) over H1—a ratio of the major length (Out_{dist}) vs. height (H1) dimensions of the mandible, interpreted as a measure of the predominant plane (sagittal vs. horizontal) of torque through the lower jaw. Capital letters refer to mandibles illustrated in Figure 4. Plotted values are means ± standard deviation. Sample sizes are given in Table 1.

Mandibular tooth row angle (TR_{angle}; Table 1; Supporting Information Fig. S2) is hypothesized to directly correspond with mandibular excursion, or distance traveled by the distalmost tooth during adduction, and inversely correspond with torque differential at equivalent TRLs. Computed values of TR_{angle} ranged from a low of 8° for *Ancistrus* sp. "longjaw" to high of 50° for *Rineloricaria lanceolata* and 51° for *Panaque albomaculatus*. Values above 25° were observed only in members of the Ancistrini genera *Panaque* (30°–51°) and *Peckoltia* (26°), the Loricariini genera *Spatuloricaria* (38°), *Rineloricaria* (50°), and *Loricaria* (36°), the Hypostomini species *Hypostomus pyrineusi* (27°), and the Farlowellini species *Farlowella amazonum* (31°). All other species were distributed more or less continuously between 11° (*Ancistrus* sp. "shortjaw") and 22° (*Hypostomus unicolor*).

DISCUSSION

When viewed in conjunction with hypotheses of phylogenetic relationships among examined taxa (Fig. 9; Rapp Py-Daniel, 1997; Sullivan et al., 2006; Armbruster, 2008), multivariate analysis of the mandibular morphofunctional parameters measured herein demonstrates that jaw diversity in modern Loricariidae is likely the result of both phylogenetic niche conservatism and repeated adaptive radiation and trophic specialization. Several lines of evidence suggest that the ancestral mandibular morphology for Loricariidae has been relatively conserved in many modern taxa and would likely occupy a portion of morphospace near PC2 = 0 (Fig. 9A) and near the center of distribution of most modern taxa at relatively high values of PC3 and PC4 (Fig. 9B). Support for this can be drawn from the similar distribution of New Genus mandibles and the phylogenetically basal position of this lineage within Ancistrini (Fig. 9C). Likewise, similar morphospatial distributions are shared by most nonspecialized (i.e., non-wood-eating and nonrheophilic) Ancistrini species, by the nonspecialized (i.e., non-wood-eating) Hypostomini species, and by the nonspecialized (i.e., non-sand-dwelling and noninsectivorous) species in subfamily Loricariinae. This region of mandibular morphospace, which is crowded with many nonspecialized loricariids, can be associated with a generalized diet of detritus and biofilm scraped from solid surfaces of wood and rock (Lujan et al., 2011).

Although a generalized, ancestral loricariid mandibular morphology has likely been conserved within many loricariid lineages, the examined taxa provide multiple examples of trophic specialization and diversification via adaptive radiation. The most striking and morphologically diverse of these is the radiation of genera within tribe Ancistrini, which exhibit a continuous but largely nonoverlapping distribution along the PC2 axis. Although Ancistrini genera near the PC2 centroid are challenging to distinguish ecologically given the current paucity of life history data, the morphospatially distant genera *Chaetostoma* and *Panaque* are, respectively, associated with specialized habitats and diets. Moreover, C and N stable isotope data from sympatric loricariid assemblages distributed across South America suggest that these fish structure trophic resources to a greater extent than can be determined via gut contents analysis alone (Lujan, 2009).

Chaetostoma are distinguished by having exceptionally wide jaws and long tooth rows with many

small teeth (Figs. 3A and 4C), which they use to forage on epilithic detritus and biofilm in relatively shallow, swift-flowing streams of the Andean piedmont (Hood et al., 2005). All but two of the ~50 recognized *Chaetostoma* species are restricted to these habitats along the flanks of the Andes Mountains (Anderson and Maldonado-Ocampo, 2011), and the two non-Andean species occupy similar habitats in rivers draining the Guiana Shield uplands of Venezuela and Brazil (Lasso and Provenzano, 1997). Six *Chaetostoma* spp. examined herein have a high degree of overlap within their uniquely occupied region of morphospace (Fig. 9E), thus reflecting a trophic morphological niche that is specialized and derived within Loricariidae, but conserved within the genus. Intriguingly, in many similar loricariid habitats that are outside the range of *Chaetostoma* (e.g., piedmont regions of the Bolivian Andes, Southeastern Brazil, portions of the Guiana and Brazilian shields), several similar jaw morphologies can be observed in a variety of distantly related loricariid genera (e.g., *Pseudancistrus pectegenitor* in the upper Orinoco River of Venezuela, *Ancistrus megalostomus* in the Beni Basin of Bolivia, and several *Hypostomus* species in Southeastern Brazil and the Brazilian Shield). These patterns suggest that in similar habitats, similar selection pressures have repeatedly driven evolutionary convergence upon *Chaetostoma*-like, wide-jawed mandibular morphologies, but that within this niche, at least as exemplified by the six sympatric *Chaetostoma* species examined here, there appears to be relatively little competitive pressure to segregate the niche in a manner reflected in mandibular morphological divergence.

In contrast, four species of the ancistrine genus *Panaque* have diversified into mutually exclusive regions of mandibular morphospace (Fig. 9F) and are known to at least partially segregate trophic resources assimilated (despite having similar gut contents; German, 2009; Lujan et al., 2011). These species have overlapping geographic distributions in the upper Amazon Basin and were collected syntopically for this study. Contiguous but largely nonoverlapping segregation of jaw functional traits, combined with the partial segregation of N isotope space (Lujan et al., in press), suggests that these wood-eating loricariids represent a geographically restricted adaptive radiation. Furthermore, specialization on a diet of wood appears to have driven convergence upon *Panaque*-like mandibular morphologies in the distantly related *Hypostomus cochliodon* group (represented herein by *H. pyrineusi*, Fig. 9G). Among the four *Hypostomus* species sampled here, only the wood-eating *H. pyrineusi* has a jaw morphology broadly overlapping that of genus *Panaque* (Fig. 9C,G), and only *H. pyrineusi* shares with *Panaque* the presence of short, highly angled rows of few, stout teeth, each having a unicuspid crown with the concave, adze-like shape of a carpentry instrument (Fig. 3D–G,K; Armbruster, 2003). These loricariids and their congeners are the only fishes known to specialize on a diet of wood; however, they are unable to assimilate wood directly and appear to be nutritionally dependent on microbes living on and in the wood (German, 2009; Lujan et al., in press).

Habitat specialization in *Chaetostoma* and dietary specialization in both *Panaque* and the *Hypostomus cochliodon* group exemplify two main categories of selection pressure that likely affect loricariid jaw evolution. Habitat and trophic specializations of the tribe Loricariini suggest that its isolation in a unique region of mandibular morphospace apart from all other taxa (Fig. 9B,D) may have been driven by selection in both of these categories. In contrast to most other loricariids examined herein, which forage by scraping food from solid substrates, species in tribe Loricariini are most commonly associated with sandy substrates, from which they separate and consume mostly aquatic invertebrates and seeds rather than biofilm (Armbruster, 2004; Melo et al., 2004). The need to separate discrete food items from loosely aggregated substrates places distinct functional demands on the oral apparatus of fishes (Weisel, 1960), and rather than scraping solid surfaces like most loricariids, loricariine species can be observed in natural habitats and in aquaria to forage by winnowing in a manner similar to catostomid suckers (Weisel, 1960) and surf perches (Drucker and Jensen, 1991). A single species among the examined Hypostomini, *Hypostomus unicolor*, shares sand-flat habitats and a similar foraging mode with members of the Loricariini. Although *H. unicolor* is distant from the Loricariini in mandibular morphospace described by PCs 3 and 4, it is the closest of all examined Hypostomini to Loricariini in the functional metrics described below (Fig. 10).

Force Intensity

The unique region of mandibular morphospace occupied by the wood-eater *Panaque* cf. *bathyphilus* is distinguished from other taxa along the PC3 axis mostly by its increased area of adductor insertion (AM_{area}; Fig. 9F; Table 3), whereas differentiation of *Panaque* and *Hypostomus pyrineusi* along the PC2 axis is driven mostly by their relatively short TRLs (Fig. 9C,G; Table 3). Together, these specializations can be interpreted as avenues toward increased force generation and force concentration that are independent of mandibular MA and can be examined together via interspecific variation in the metric AM_{area}/TRL^2 (Fig. 10 and Supporting Information Fig. S1). Specialized wood-eating loricariids have AM_{area}/TRL^2 values higher than all other species except *Peckoltia bachi* (represented herein by only two individuals). The force

TABLE 3. Summary of eigenvalues, eigenvectors, and % variance explained by each principal component (PC) in a PC analysis of six morphometrics measured from the mandibles of 377 individuals and 25 species of Loricariidae collected in the upper Amazon Basin of northern Peru (Table 1)

	PC1	PC2	PC3	PC4	PC5	PC6
Eigenvalue	54.1	7.5	1.2	0.2	0.1	0.0
% variance	85.7	11.9	2.0	0.3	0.1	0.1
Cumulative %	85.7	97.6	99.6	99.8	99.9	100.0
			Eigenvectors			
AM_{area}	**0.920**	−0.059	**−0.384**	−0.039	0.002	−0.026
H1	0.165	−0.134	0.356	**0.838**	0.001	**−0.355**
In	**0.102**	0.042	0.144	0.317	0.096	**0.926**
Out_{dist}	0.266	0.100	**0.648**	−0.297	**−0.641**	0.034
Out_{prox}	0.158	**−0.475**	0.489	**−0.326**	**0.636**	−0.026
TRL	0.140	**0.861**	0.217	−0.034	0.420	−0.120

Maximum and minimum values are given in bold.

concentration achieved by a large adductor muscle and a short TRL is likely multiplied among the wood-eating species via reductions in tooth number. Only the specialized wood eaters (not *P. bachi*) have specialized teeth that are stout and few in number relative to most other loricariids, resulting in a concentration of force not just along a shorter tooth row but also at fewer more rigid points along the tooth row. *Peckoltia bachi* is not known to have any dietary specializations, but the trophic ecologies of *Peckoltia* spp. remain largely unstudied.

Many herbivores and detritivores are known to compensate for their nutrient-deficient diets in part by increasing consumption rate and food volume (Horn and Messer, 1992). In the loricariids for which gut passage rates have been measured (*Ancistrus triradiatus* and *Panaque nigrolineatus*), ingesta passing through intestines with lengths several times greater than standard body lengths had very short residence times ranging from 40 min to 4 h (Hood et al., 2005; German, 2009). Given these gut passage rates and the known specialization of loricariid intestinal physiologies for rapid assimilation of easily digested molecules released during microbial degradation of detritus (German, 2009), they likely strive to maximize food ingestion rates and volumes given the limitation that foods must first be gathered and separated from surfaces. Generalist consumers of flocculent detritus or loosely attached periphyton would therefore be predicted to have low values of the metric AM_{area}/TRL^2 indicative of force distribution. Among the species examined, *Chaetostoma* spp. have some of the lowest AM_{area}/TRL^2 values (Fig. 10 and Supporting Information Fig. S1) and some of the longest tooth rows of any loricariid (Fig. 3C); they are also known to feed largely upon detritus that accumulates on the surface of stream substrates (Saul, 1975; Kramer and Bryant, 1995).

Traditional Metrics of MA

Relative distances between areas of force-in or force-out and axes of rotation determine a rotating system's MA or the degree to which the system favors force vs. speed. In an absolute sense, values below 1 favor speed (speed and displacement are increased and force is decreased in comparison to what enters the system); values above 1 favor strength (force is increased and speed and displacement decreased); and values of 1 represent balanced systems in which force, speed, and displacement into and out of the system are equal. All reported teleost MA values are below 1 and range from 0.04 in piscivorous fishes such as needlefishes (Belonidae) to 0.68 for coralivous parrotfishes (Scaridae; Westneat, 2004); therefore, relative to a balanced system of jaw closure, adductor mandibulae force is reduced and jaw speed and displacement are increased at the distalmost tooth of all examined teleosts regardless of diet.

The heuristic strength of the MA metric lies in the complex functional tradeoffs that this single number can allude to, including not only bite force and speed but also gape size and degree of jaw protrusion. The observation, though, that jaws of even the most durophagous teleosts favor speed and displacement over force suggests that there may be a limit to the explanatory value of MA, especially among durophagous fishes. We suggest that especially for durophagous fishes, additional properties of rotating systems should be considered, and the Loricariidae are an excellent group in which to investigate the importance of these additional properties. Among loricariids, it can be difficult to justify the tradeoffs required to maintain jaws with MA less than 1. Loricariid diets are entirely benthic and frequently nonliving (detritus and wood), sessile (algae, diatoms, and sponge), or slow moving (e.g., aquatic Trichoptera and Lepidoptera larvae, snails), suggesting that loricariid

jaws rarely need to be fast to capture prey. Moreover, loricariid gut contents typically consist of very small, loosely aggregated particles, suggesting that gape limitations are rare and loricariid mandibular displacement need not be maximized for prey ingestion (loricariid pharyngeal jaws are typically weak, so the small size of gut contents should be an accurate indicator of size at ingestion).

Despite having diets and foraging modes that would seem to make especially high MA values evolutionarily available, even the most durophagous of loricariids (the wood-eating *Panaque* spp.) exhibit a maximum MA of 0.41. Moreover, wood-eating loricariids are distinguished by having proximal teeth that are displaced distally relative to the jaw joint, creating a highly angled tooth row in which all teeth have similarly long output lever arms and reduced MA. If the evolutionary specialization of wood-eating loricariids led to mandibles that maximize strength over speed, the tooth row would be expected to shift closer to the jaw joint, as with the carnasial and molar chewing teeth of carnivorous and ungulate mammals, respectively (Greaves, 1978, 1983). Unlike tetrapod jaws, fish jaws appear to be evolutionarily constrained to favor speed. Wood-eater jaw function might therefore be compared to that of a carpentry rasp, which removes shallow surface layers of wood by moving rapidly with relatively weak normal (downward) forces. Support for this analogy comes from microscopic studies of *Panaque* gut contents (Schaefer and Stewart, 1993; German, 2009), which reveal wood pieces that are small, like chips produced by a rasp. Long curls of wood that are produced when other carpentry tools (e.g., gouges and draw knives) are slowly and forcefully applied to wood have not been observed in stomachs of wood-eating loricariids.

Novel Metrics of Jaw Function

Any calculation of loricariid mandibular MA using in-lever and out-lever arms that are traditionally defined must account for the almost parallel orientation of these parameters with respect to the transverse axis around which the mandible rotates (Axis 1, Fig. 8; Adriaens et al., 2009). Only the component of a given lever that is perpendicular to its rotational axis can control MA of the rotating body. Although the complex geometry and rotational freedom of loricariid mandibles largely prevents direct identification and measurement of lever arm dimensions most relevant to Axis 1, these dimensions are illustrated in the rotating cone model as radius 1 (r_1, input) and radius 2 (r_2, output; Fig. 8). Radii are by definition perpendicular to the axis of rotation, and r_1 and r_2 are, respectively, defined as the distances from this axis to the regions of force-in and force-out. As such, they are essentially the sagittal components of the traditionally defined in-lever and distalmost out-lever arms.

Unfortunately, direct measurement of r_1 and r_2 is impossible without knowing the three-dimensional position of Axis 1 relative to points where forces enter and leave the mandible. Instead, we hypothesize that the parameter H1 (Fig. 6) might be treated as a correlate of variation in r_1. H1 is defined as perpendicular to the distalmost out-lever arm, which was consistently the most transversely oriented parameter. H1 measures distance from this out-lever to the height of the coronoid arch, on which inserts the adductor mandibulae, supporting H1's similarity to the idealized in-lever parameter r_1. For the idealized out-lever parameter r_2, we hypothesize that the metric TR_{angle} might serve as a proxy. As illustrated in Figure 8, TR_{angle} is related to the hypothesized maximum excursion of mandibular teeth. Mandibles with higher TR_{angle} not only displace proximal teeth more distally from the anguloarticular joint but also align the tooth more perpendicularly relative to Axis 1. This orientation would be predicted to increase protrusion of the tooth row and correspond with an increase in r_2.

Directly relating H1 and TR_{angle} to each other to evaluate the potential for intraspecific variation in MA must be done with caution because of the imprecision inherent to both metrics and the likelihood of intraspecific variation in their relative position and orientation. We did, however, examine the relationship between the putative input lever H1 and TRL (H1/TRL, Fig. 11). This analysis recovered the wood-eating loricariids (plus the non-wood-eater *Peckoltia bachi*) as a cluster of elevated values, presumably associated with both a long input lever to maximize MA and a short tooth row to concentrate forces exiting the mandible. The metric H1/TRL also shows a strong linear relationship with AM_{area}/TRL^2, although this is to be expected given the shared denominators and close relationship between the height of the coronoid arch and the area of adductor mandibular insertion.

Adriaens et al. (2009) demonstrated that rotation of the loricariid jaw has both sagittal and horizontal components (i.e., rotational Axes 1 and 2, Fig. 8). We hypothesize that loricariids may emphasize one of these rotational axes over the other by varying mandibular morphological dimensions in a manner that shifts the predominant plane of torque. To assess whether a given species produces mandibular torque predominantly in sagittal or horizontal planes, we calculated $Out_{dist}/H1$ (Fig. 11). Among the Loricariini, relatively large Out_{dist} values indicate that teeth are positioned relatively far from the mandibular joint in the horizontal plane, whereas low H1 values indicate that insertion of the adductor mandibulae is relatively close to the rotational axis in the sagittal plane.

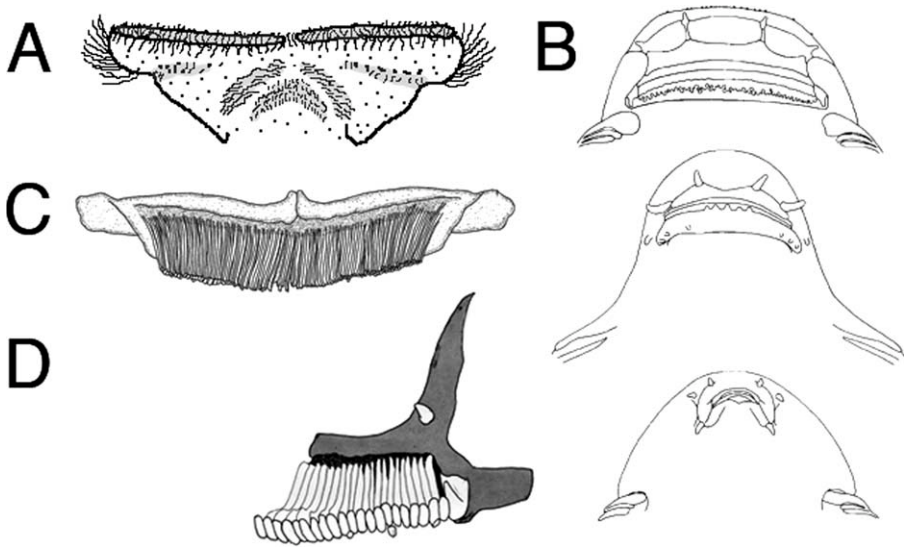

Fig. 12. Examples from outside Loricariidae of broad, truncate jaws that support many small teeth or bristles and are used by a variety of aquatic taxa to scrape algae or gather detritus from submerged surfaces: **A**: *Wormaldia occipitalis*, Trichoptera, Insecta (labrum in dorsal view modified from Satija and Satija, 1959), **B**: various genera, Gastromyzontinae, Cypriniformes (snout in ventral view modified from Roberts, 1989), **C**: *Euchilichthys royauxi*, Atopochilini, Siluriformes (lower jaw in anterior view; Vigliotta, 2008), and **D**: *Ecsenius bicolor*, Salariinae, Blenniidae (left lower jaw ramus in anterior view; Springer, 1988). See Figure 2 for similar spectrum of jaw morphologies in Loricariidae.

This mandibular geometry suggests that a Loricariini mandible experiences relatively less torque in the sagittal plane than in the horizontal plane. In contrast, durophagous species have high Out_{dist} values coupled with high H1 values, suggesting a more balanced system with both torque and rotation predominantly in the sagittal plane. When combined with a predictor of force allocation (AM_{area}/TRL^2), it is clear that the sagittal torque transmitted through wood-eater mandibles increases both as a function of $Out_{dist}/H1$ and AM_{area} and that the resulting mandibular adduction forces are concentrated on smaller substrate areas via reduced TRL and fewer teeth.

Comparisons With Other Herbivorous Fishes

The distinctively broad, truncate tooth rows of *Chaetostoma* and many other loricariids can be placed along a spectrum of jaw morphologies parallel to that seen among a wide variety of other aquatic herbivorous–detritivorous, surface-scraping grazers. Caddisfly larvae (Trichoptera), which are among the most ubiquitous metazoan grazers in temperate streams, have a broad, bristly labrum with which they collect algae and detritus from stream surfaces (Fig. 12A; Arens, 1989, 1990, 1994). In Asian tropical streams, the Gastromyzontinae (Cypriniformes) exhibit a range of jaw widths (Fig. 12B) that Roberts (1989) associated with a dietary spectrum from carnivory (narrow) to herbivory (wide). And in the tropical rivers of Africa, the surface-scraping catfish tribe Atopochilini (Mochokidae; Fig. 12C; Vigliotta, 2008) is remarkably convergent on members of the Loricariidae. All atopochilines have very wide jaws that function within a fleshy labial disk, and the tribe is at least partially diagnosed by having a ventral mesethmoid condyle for articulation with premaxillae, although atopochiline jaw function and trophic ecology is even less studied than the Loricariidae. In marine systems, the blenniid genus *Ecsenius* (Fig. 12D; Springer, 1988) and the squamipinnes group (including the surgeonfishes, Acanthuridae, and butterflyfishes, Chaetodontidae; Konow et al., 2008) are abundant on reefs and include many herbivorous and detritivorous species with relatively broad, truncate snouts comparable to the jaws of loricariids. As all of these organisms form the base of fish food webs in each of their respective habitats, greater effort should be expended to understand the functional, ecological, and evolutionary consequences of their often highly derived jaw mechanisms.

ACKNOWLEDGMENTS

The authors gratefully acknowledge Kevin Conway, Craig Guyer, Jack Feminella, Dennis Devries, Adam Summers, and anonymous reviewers for helpful discussions and comments on previous versions of this manuscript; Alex Flecker and Donovan German for financial and logistical support of fieldwork in Peru; Krista Capps, Darwin Osorio, Donald Taphorn, and David Werneke for assistance in collecting specimens and for collection management; Hernan Ortega and Blanca Rengifo

(MUSM), Peruvian authorities (IMARPE), and the Aguaruna indigenous people (ODECOFRO) for permit and logistical support of fieldwork; and Julian Humphries (Digimorph, University of Texas, Austin) and Kyle Luckenbill (Academy of Natural Sciences, Philadelphia) for assistance with CT scans and data manipulation. This project is part of the Planetary Biodiversity Inventory: All Catfish Species (Siluriformes; NSF DEB-0315963). For salary support during the completion of this manuscript, NKL thanks Kirk Winemiller and the Estate of George and Carolyn Kelso via the International Sportfish Fund.

LITERATURE CITED

Adriaens D, Geerinckx T, Vlassenbroeck J, Van Hoorebeke L, Herrel A. 2009. Extensive jaw mobility in suckermouth armored catfishes (Loricariidae): A morphological and kinematic analysis of substrate scraping mode of feeding. Physiol Biochem Zool 82:51–62.

Anderson EP, Maldonado-Ocampo JA. 2011. A regional perspective on the diversity and conservation of tropical Andean fishes. Conserv Biol 25:30–39.

Arens W. 1989. Comparative functional morphology of the mouthparts of stream animals feeding on epilithic algae. Arch für Hydrobiol 83 (Suppl):253–354.

Arens W. 1990. Wear and tear on mouthparts: A critical problem in stream animals feeding on epilithic algae. Can J Zool 68:1896–1914.

Arens W. 1994. Striking convergence in the mouthpart evolution of stream-living algae grazers. J Zool Syst Evol Res 32:319–343.

Armbruster JW. 2004. Phylogenetic relationships of the suckermouth armoured catfishes (Loricariidae) with emphasis on the Hypostominae and the Ancistrinae. Zool J Linn Soc 141:1–80.

Armbruster JW. 2008. The genus Peckoltia with the description of two new species and a reanalysis of the phylogeny of the genera of the Hypostominae (Siluriformes: Loricariidae). Zootaxa 1822:1–76.

Delariva RL, Agostinho AA. 2001. Relationships between morphology and diets of six neotropical loricariids. J Fish Biol 58:832–847.

Drucker EG, Jensen JS. 1991. Functional analysis of a specialized prey processing behavior: Winnowing by surfperches (Teleostei: Embiotocidae). J Morphol 210:267–287.

Fugi R, Agostinho AA, Hahn NS. 2001. Trophic morphology of five benthic-feeding fish species of a tropical floodplain. Rev Bras Biol 61:27–33.

Geerinckx T. 2006. Ontogeny and functional morphology of a highly specialized trophic apparatus: A case study of neotropical suckermouth armoured catfishes (Loricariidae, Siluriformes). D. Phil. Thesis, University of Gent, Gent, Belgium.

Geerinckx T, Brunain M, Herrel A, Aerts P, Adriaens D. 2007a. A head with a suckermouth: A functional-morphological study of the head of the suckermouth catfish Ancistrus cf. triradiatus (Loricariidae, Siluriformes). Belg J Zool 137:47–66.

Geerinckx T, De Poorter J, Adriaens D. 2007b. Morphology and development of teeth and epidermal brushes in loricariid catfishes. J Morphol 268:805–814.

German DP. 2009. Inside the guts of wood-eating catfishes: Can they digest wood? J Comp Physiol B 179:1011–1023.

Greaves WS. 1978. The jaw lever system in ungulates: A new model. J Zool (London) 184:271–285.

Greaves WS. 1983. A functional analysis of carnassial biting. Biol J Linn Soc 20:353–363.

Hood JM, Vanni MJ, Flecker AS. 2005. Nutrient recycling by two phosphorus rich grazing catfish: The potential for phosphorus-limitation of fish growth. Oecologia 146:247–257.

Horn MH, Messer KS. 1992. Fish guts as chemical reactors: A model of the alimentary canals of marine herbivorous fishes. Mar Biol 113:527–535.

Konow N, Bellwood DR, Wainwright PC, Kerr AM. 2008. Evolution of novel jaw joints promote trophic diversity in coral reef fishes. Biol J Linn Soc 93:545–555.

Kramer DL, Bryant MJ. 1995. Intestine length in the fishes of a tropical stream. II. Relationships to diet—The long and short of a convoluted issue. Environ Biol Fish 42:129–141.

Lasso CA, Provenzano F. 1997. *Chaetostoma vasquezi*, nueva especie de corroncho del Escudo de Guyana, estado Bolívar, Venezuela (Siluroidei: Loricariidae): Descripción y consideraciones biogeográficas. Memoria Sociedad de Ciencias Naturales La Salle 57:53–65.

Lauder GV. 1982. Historical biology and the problem of design. J Theor Biol 97:57–67.

Lujan NK. 2009. Jaw morpho-functional diversity, trophic ecology, and historical biogeography of the neotropical suckermouth armored catfishes (Siluriformes, Loricariidae). Ph.D. Dissertation, Auburn University, Auburn, AL.

Lujan NK, German DP, Winemiller KO. 2011. Do wood grazing fishes partition their niche? Morphological and isotopic evidence for trophic segregation in neotropical Loricariidae. Funct Ecol published online 1 July 2011.

Melo CE, Arruda F, Pinto-Silva V. 2004. Feeding habits of fish from a stream in the savanna of Central Brazil, Araguaia Basin. Neotrop Ichthyol 2:37–44.

Mérona B, Hugueny B, Tejerina-Garro FL. 2008. Diet-morphology relationship in a fish assemblage from a medium-sized river of French Guiana: The effect of species taxonomic proximity. Aquat Living Resour 21:171–184.

Muller S, Weber C. 1992. Les dents des sous-familles Hypostominae et Ancistrinae (Pisces, Siluriformes, Loricariidae) et leur valeur taxonomique. Revue Suisse de Zool 99:747–754.

Rapp Py-Daniel L. 1997. Phylogeny of the neotropical armored catfishes of the subfamily Loricariinae (Siluriformes: Loricariidae). D. Phil. Thesis, University of Arizona, Tucson, AZ.

Reis RE, Kullander SO, Ferraris CJ Jr. 2003. Check List of the Freshwater Fishes of South and Central America. Porto Alegre: EDIPUCRS.

Roberts TR. 1989. The freshwater fishes of Western Borneo (Kalimantan Barat, Indonesia). Memoirs Calif Acad Sci 14:1–210.

Satija RC, Satija GR. 1959. Food in relation to mouth-parts and alimentary canal of *Wormaldia occipitalis* Pictet (Philopotamidae) larvae. Res Bull (N.S.) Punjab Univ 10:169–178.

Saul WG. 1975. An ecological study of fishes at a site in upper Amazonian Ecuador. Proc Acad Nat Sci Phila 127:93–134.

Schaefer SA, Lauder GV. 1986. Historical transformation of functional design: Evolutionary morphology of feeding mechanisms in loricarioid catfishes. Syst Zool 35:489–508.

Schaefer SA, Lauder GV. 1996. Testing historical hypotheses of morphological change: Biomechanical decoupling in loricarioid catfishes. Evolution 50:1661–1675.

Schaefer SA, Stewart DJ. 1993. Systematics of the Panaque dentex species group (Siluriformes: Loricariidae), wood-eating armored catfishes from tropical South America. Ichthyol Explor Freshwaters 4:309–342.

Springer VG. 1988. The Indo-Pacific blenniid fish genus Ecsenius. Smithson Contrib Zool 465:1–134.

Sullivan JP, Lundberg JG, Hardman M. 2006. A phylogenetic analysis of the major groups of catfishes (Teleostei: Siluriforms) using rag1 and rag2 nuclear gene sequences. Mol Phylogenet Evol 41:636–662.

Vigliotta TR. 2008. A phylogenetic study of the African catfish family Mochokidae (Osteichthyes, Ostariophysi, Siluriformes), with a key to genera. Proc Acad Nat Sci Phila 157:73–136.

Weisel GF. 1960. The osteocranium of the catostomid fish, *Catostomus macrocheilus*: A study in adaptation and natural relationships. J Morphol 106:109–129.

Westneat, MW. 2003. A biomechanical model for analysis of muscle force, power output and lower jaw motion in fishes. Journal of Theoretical Biology 223:269–281.

Westneat MW. 2004. Evolution of levers and linkages in the feeding mechanisms of fishes. Integr Comp Biol 44:378–389.